J Appl Electrochem (2013) 43:927–937
DOI 10.1007/s10800-013-0578-6

ORIGINAL PAPER

High electrocatalysis of ethylene glycol oxidation based on nickel particles electrodeposited into poly (*m*-toluidine)/Triton X-100 composite

Reza Ojani · Jahan-Bakhsh Raoof · Mona Goli · Ali Alinezhad

Received: 19 March 2013 / Accepted: 25 June 2013 / Published online: 9 July 2013

Abstract Poly (*m*-toluidine) (PMT) was formed by successive cyclic voltammetry in a monomer solution containing Triton X-100 (TX-100) at the surface of carbon paste electrode (CPE). Nickel was then incorporated into the polymer by electrodeposition of Ni(II) from $NiSO_4$ acidic solution. The electrochemical behavior of this modified electrode (Ni/PMT(TX-100)/MCPE) was investigated in the electrooxidation of ethylene glycol (EG) using cyclic voltammetry and chronoamperometry techniques. Among the electrodes [Ni/PMT(TX-100)/MCPE, Ni/PMT/MCPE, Ni/MCPE, PMT(TX-100)/MCPE, and CPE] used in this study, Ni/PMT(TX-100)/MCPE showed the most effective catalytic activity. The effects of various parameters such as film thickness, electrodepositing time, TX-100 concentration, MT concentration, and EG concentration were investigated on the electrocatalytic oxidation of EG at the surface of Ni/PMT(TX-100)/MCPE. The catalytic rate constant (k) for EG oxidation was also calculated to be 2.1×10^6 cm^3 mol^{-1} s^{-1} using a chronoamperometric method.

R. Ojani (✉)
Electroanalytical Chemistry Research Laboratory, Department of Analytical Chemistry, Faculty of Chemistry, University of Mazandaran, 4741695447 Babolsar, Iran
e-mail: fer-o@umz.ac.ir

J.-B. Raoof · M. Goli · A. Alinezhad
Faculty of Chemistry, University of Mazandaran, Babolsar, Iran
e-mail: j.raoof@umz.ac.ir

M. Goli
e-mail: mona_g4485@yahoo.com

A. Alinezhad
e-mail: alinejad@umz.ac.ir

Keywords Triton X-100 · Nickel particles · Electrocatalytic oxidation · Ethylene glycol · Poly (*m*-toluidine)

1 Introduction

Fuel cells are one of the most important technologies which have recently gained researchers' growing attention. This is mainly due to their high efficiency and environmentally friendly technology for energy conversion. Several substances such as formic acid, methanol, and ethylene glycol have been studied as model fuels [1]. Ethylene glycol, because of its higher energy density, lower toxicity, lower flammability, and lower permeation through the polymer electrolyte membrane compared to methanol and formic acid, has been considered for direct alcohol fuel cell applications [2–6]. Therefore, the electrooxidation of EG has attracted considerable interest in recent years, both from practical and from fundamental points of view [7–15]. On the other hand, the concept of modified electrodes is an exciting development in the field of electroanalytical chemistry. Recently, modified electrodes with metallic microparticles electrodeposited into the polymeric matrix have been used for determining various species [16–18]. Although various metallic microparticles can be used for dispersion in thin organic films, Ni microparticles, due to its cost-effectiveness, has gained greater interest for alcohol electrooxidation as a catalyst. Ni is commonly used as an electrocatalyst for both anodic and cathodic reactions in organic synthesis and aqueous electrolysis [19–23]. Several investigations on the electrooxidation of alcohols on Ni have already been reported [24, 25].

In the present study, poly (*m*-toluidine) (PMT) was prepared by electropolymerization of monomer solution in

the presence of TX-100 at the surface of carbon paste electrode. Ni was then incorporated into the polymer by electrodeposition of Ni(II) from $NiSO_4$ acidic solution using electrolysis at fixed potential. Therefore, poly (*m*-toluidine)/TX-100-modified CPE, which is a conductive organic matrix was prepared and allowed a better dispersion of Ni particles as a catalyst for EG electrooxidation.

2 Experimental

2.1 Reagents and materials

The solvent used in this study was double-distilled water. Sulfuric acid and sodium hydroxide (from Merck) were used as the supporting electrolytes. $NiSO_4$ $6H_2O$ (from Fluka), *m*-toluidine, EG, and TX-100 (from Merck) were used as received. High-viscosity paraffin (density 0.88 g cm^{-3}) (from Fluka) was used as the pasting liquid for the carbon paste electrode. Graphite powder (particle diameter of 0.10 mm) (from Merck) was used as the working electrode substrate. All other reagents were of analytical grade.

2.2 Instrumentation

Electrochemical experiments were performed using a potentiostat/galvanostat (μ-Autolab TYPE III, Eco Chemie BV, Netherlands) coupled with a Pentium IV personal computer. A platinum disk was used as the auxiliary electrode. A carbon paste electrode as working electrode and a double junction Ag|AgCl||KCl (3 M) electrode as the reference electrode were utilized.

2.3 Working electrode preparation

First, carbon paste was prepared by hand-mixing of paraffin and graphite powder by means of a mortar and pestle. Then, the resultant paste was inserted in the bottom of a glass tube (internal radius of 2.2 mm). The electrical connection was implemented by copper wire lead matched into the glass tube.

A fresh electrode surface was generated rapidly by extruding a small plug of the paste by a stainless steel rod and smoothing the resulting surface on white paper until a smooth shiny surface was observed.

The modification of the carbon paste electrode was performed in three steps:

I. Electropolymerization of *m*-toluidine monomer by potential cycling (ten cycles at a scan rate of 50 mV s^{-1}) between 0.0 and 1.2 V versus Ag|AgCl||KCl (3 M) in aqueous solution containing 0.5 M H_2SO_4, 6 mM *m*-toluidine monomer, and 6 mM TX-100.
II. Deposition of Ni particles into PMT(TX-100) films by electroreduction of 1.5 M $NiSO_4$ in 1.0 M H_2SO_4 solution. Electroreduction step was carried out using chronoamperometry technique (−1.0 V vs. Ag|AgCl||KCl (3 M) for 900 s).
III. Afterward, the electrode was removed and rinsed with water and the sides were wiped with soft tissue paper. The prepared electrode was conditioned in 0.1 M NaOH solution by potential cycling between 0.0 and 0.8 V versus reference electrode at a potential sweep rate of 50 mV s^{-1} for ten cycles of potential. The parameters were obtained experimentally as optimum values for complete transformation of Ni/PMT(TX-100) to $Ni(OH)_2$/PMT(TX-100) and maximum activation of electrode surface toward the electrocatalytic oxidation of EG.

3 Results and discussion

3.1 Electrochemical behavior of PMT(TX-100)/MCPE

The PMT film was prepared on the surface of carbon paste electrode in the absence and in the presence of TX-100. The cyclic voltammetry behavior of PMT/MCPE was compared to that of PMT(TX-100)/MCPE in Fig. 1. PMT/TX-100 films showed considerably higher redox current than the normal PMT film which reflects the effective active surface areas that are accessible to the electrolytes at PMT(TX-100)/MCPE. Apparently, the porous PMT/TX-100 films have more effective surface areas. This improvement in doping–undoping rate results from the increase in the surface area and porous structure which are of benefit to the ion diffusion and migration as reported previously [26–32]. Furthermore, the PMT/TX-100 film showed a large background current, attributed to the large surface area of porous structure immobilized on the surface of CPE.

3.2 Electrochemical impedance spectroscopy studies

Electrochemical impedance spectroscopy is an effective tool for studying the interface properties of surface-modified electrodes. The typical impedance spectrum (presented in the form of the Nyquist plot) includes a semicircle portion at higher frequencies corresponding to the limited electron-transfer process and a linear part at lower frequency range representing the diffusion-limited process. The semicircle diameter in the impedance spectrum equals the electron-transfer resistance, R_{et}. This resistance controls the electron-transfer kinetics of the redox probe at the electrode interface. Therefore, R_{et} can be used to describe the interface properties of the electrode.

The Nyquist diagrams of CPE (curve a), PMT/MCPE (curve *b*), and PMT(TX-100)/MCPE (curve *c*) in the presence of 1.0 mM $K_3[Fe(CN)_6]/K_4[Fe(CN)_6]$ (1:1) + 0.1 M KCl solution are shown in Fig. 2. As shown in this figure, the value of charge-transfer resistance of PMT(TX-100)/MCPE is much smaller than that of PMT/MCPE and CPE indicating a faster electron-transfer process on polymeric-modified electrode in the presence of surfactant than that on bare CPE and PMT/MCPE. This may be attributed, on one hand, to the higher real surface area of PMT(TX-100)/MCPE and, on the other hand, to the positively charged polymeric skeletons immobilized on the electrode surface that had an attraction force to $[Fe(CN)_6]^{3-/4-}$ anion. Therefore, the charge-transfer resistance of $[Fe(CN)_6]^{3-/4-}$ at the electrode surface decreased significantly. The Randles circuit was chosen to fit the impedance data obtained (Inset Fig. 2).

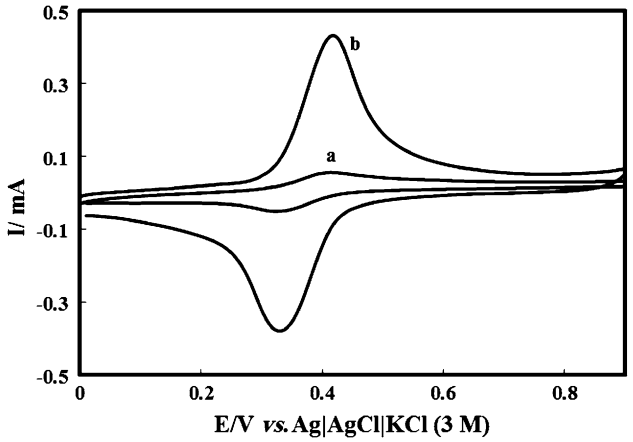

Fig. 1 Cyclic voltammograms of PMT/MCPE (*a*) and PMT(TX-100)/MCPE (*b*) in 0.5 M H_2SO_4 solution, $\upsilon = 50$ mV s^{-1}

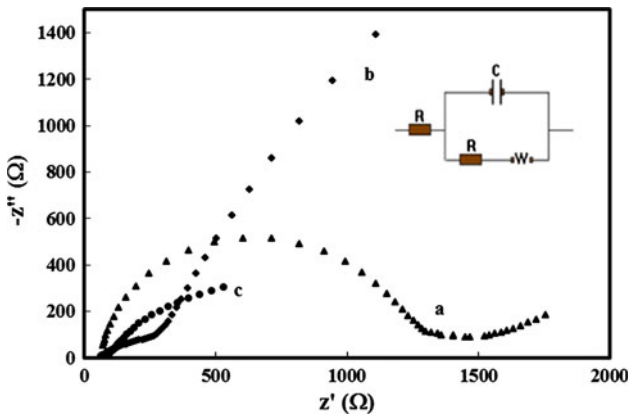

Fig. 2 Niquist plots of the Faradic impedance measurements of a 1.0 mM solution of $K_3[Fe(CN)_6]/K_4[Fe(CN)_6$ and 0.1 M KCl performed on *a* CPE, *b* PMT/MCPE, and *c* PMT(TX-100)/MCPE at bias potential 0.14 V and frequency between 10000.0 and 0.1. *Inset* the Randles circuit that was chosen for EIS

3.3 Electrode composition and Electrochemical behavior of $Ni(OH)_2$/PMT(TX-100)/MCPE

A typical energy-dispersive spectroscopy (EDS) for determination of bulk composition of the Ni/PMT(TX-100)/MCPE is presented in Fig. 3. From the EDS results shown in this figure, Ni and C are the major elements. Oxygen may come from the surfactant used in the electropolymerization of MT monomer or working electrolyte solution.

After incorporating Ni into the polymer backbone, the polarization behavior was examined in 0.1 M of NaOH for Ni/PMT(TX-100)/MCPE using cyclic voltammetry. This technique allows the formation of oxide film in parallel to inspection of the electrochemical reactivity of the surface [33]. Voltammograms were recorded by cycling the potential between 0.0 and 0.8 V at 50 mV s^{-1} until stable voltammograms were obtained (Fig. 4). Moreover, the electrochemical behavior of the PMT(TX-100)/MCPE and Ni/PMT(TX-100)/MCPE were examined in 0.1 M of NaOH solution using cyclic voltammetry (Inset Fig. 4). It is clear that neither oxidation nor reduction happened on the PMT(TX-100)/MCPE whereas well-defined redox peaks were observed on the Ni/PMT(TX-100)/MCPE. These well-defined redox peaks that appeared at 0.46 and 0.28 V could be attributed to the oxidation of $Ni(OH)_2$–NiOOH as well as the reduction of NiOOH–$Ni(OH)_2$.

The surface coverage, Γ, of the immobilized active substrate [Ni(II)] in the films can be calculated from the charge under the current–potential curve (Inset Fig. 4) with correction for the baseline ($\Gamma = Q/nFA$). The value of Γ for Ni/PMT(TX-100)/MCPE obtained 2.4×10^{-7} mol cm^{-2}.

The effect of scan rate was also examined (Fig. 5). It was found that with an increase in potential scan rate, the anodic peak potentials shift to more positive and the cathodic peak potentials shift to less positive values. The anodic and cathodic peak currents depend on the square

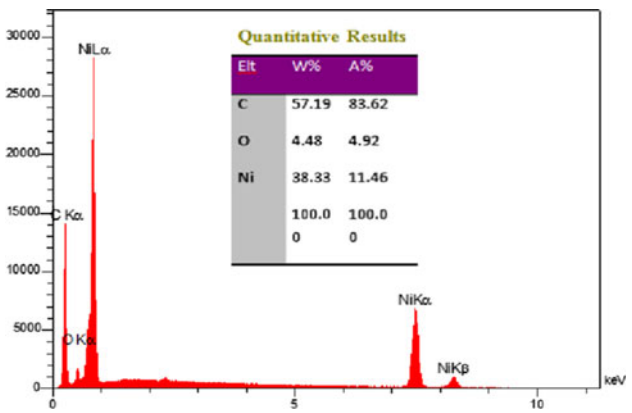

Fig. 3 Energy-dispersive spectrum (EDS) of the Ni/PMT(TX-100)MCPE

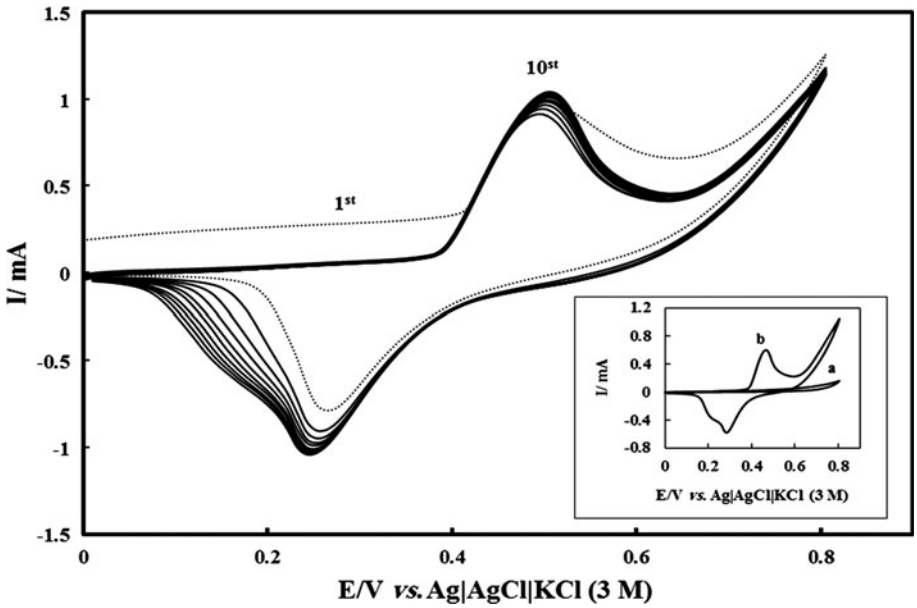

Fig. 4 Cyclic polarization behavior of Ni/PMT(TX-100)/MCPE in 0.1 M of NaOH solution at anodic potentials, $\upsilon = 50$ mV s^{-1}. *Inset* electrochemical responses of electrodes: *a* PMT(TX-100)/MCPE and *b* Ni/PMT(TX-100)/MCPE after anodic polarization

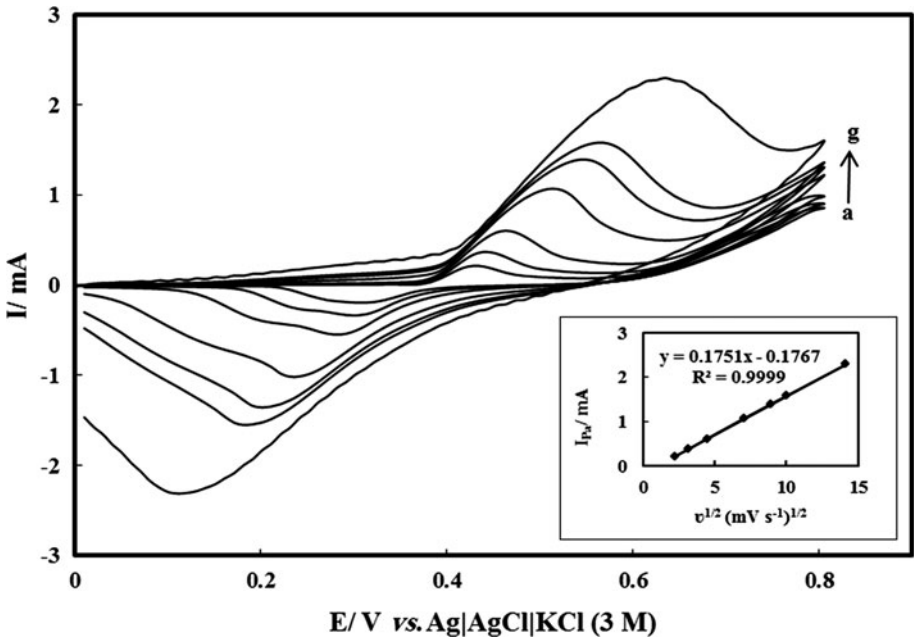

Fig. 5 Scan rate dependence of the peak current for Ni/PMT(TX-100)/MCPE in 0.1 M of NaOH solution, scan rates from inner to outer are: 5, 10, 20, 50, 80, 100, and 200 mV s^{-1}, respectively. *Inset* plot of I_{pa} versus $\upsilon^{1/2}$

root of the potential scan rate, signifying the dominance of a diffusion process as the rate-limiting step in the total redox transition of the modifier film (Inset Fig. 5). This limiting diffusion process was also reported for other Ni-modified electrodes [34, 35].

3.4 Electrocatalytic oxidation of EG at Ni/PMT(TX-100)/MCPE

The cyclic voltammograms of the CPE, PMT(TX-100)/MCPE, Ni/MCPE, Ni/PMT/MCPE, and Ni/PMT(TX-100)/MCPE in the presence of 0.04 M of EG and 0.1 M of NaOH at the scan rate of 20 mV s^{-1} presented in Fig. 6. Also, inset Fig. 6 shows the electrochemical behavior of Ni/PMT(TX-100)/MCPE in the absence and in the presence of EG. This typical behavior expected for mediated oxidation is as follows:

$$\text{E: } Ni(OH)_2 + OH^- \rightleftarrows NiOOH + H_2O + e^- \quad (1)$$

$$\text{C}' : NiOOH + EG \rightarrow Ni(OH)_2 + \text{product} \quad (2)$$

It is clear that there is a remarkable enhancement in the anodic peak current for EG oxidation at the surface of Ni/PMT(TX-100)/MCPE [Inset Fig. 6 (curve *b*)]. The difference in redox currents reflects the effective active surface

areas that are accessible to the electrolytes. Apparently, the porous PMT(TX-100) has more effective surface areas. These observations can explain clearly the role of the PMT(TX-100) on the enhancement of electrocatalytic oxidation currents of EG. Indeed, the PMT(TX-100) is a good and proper bed for immobilization of Ni particles. It seems that the main and plausible reason for such an enhancement is the formation of a polymer film backbone at the surface of CPE that provides the facile arrival of EG on Ni catalytic centers as reported previously [36].

3.5 Chronoamperometric studies

Chronoamperometry as well as cyclic voltammetry has been employed for the investigation of processes occurring via EC′ mechanism [37]. Double-step chronoamperograms

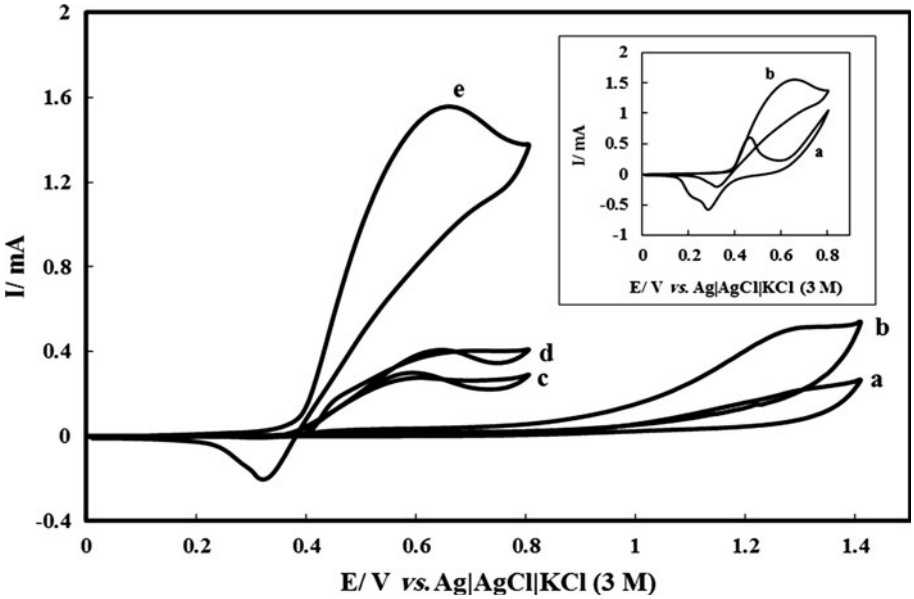

Fig. 6 Cyclic voltammograms of *a* CPE, *b* PMT(TX-100)/MCPE, *c* Ni/MCPE, *d* Ni/PMT/MCPE, and *e* Ni/PMT(TX-100)/MCPE in 0.1 M NaOH + 0.04 M EG, $\upsilon = 20$ mV s^{-1}. *Inset* electrochemical responses of Ni/PMT(TX-100)/MCPE in 0.1 M NaOH *a* in the absence and *b* in the presence of 0.04 M EG, $\upsilon = 20$ mV s^{-1}

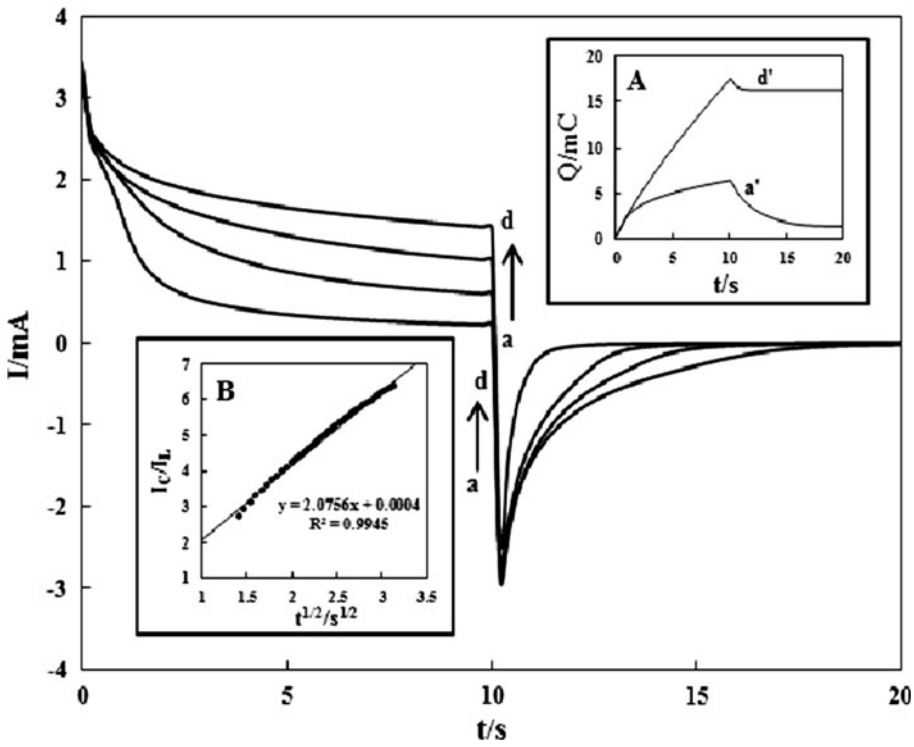

Fig. 7 Double-step chronoamperograms of Ni/PMT(TX-100)/MCPE in 0.1 M of NaOH solution with different concentrations of EG: *a* 0.00, *b* 0.01, *c* 0.02, and *d* 0.04 M. *Inset* **A** plot of Q versus t derived from the data of chronoaprograms of *a* and *d*. *Inset* **B** plot of I_C/I_L versus $t^{1/2}$ derived from the data of chronoamperograms *a* and *d*

were recorded by setting the working electrode potential at desired values.

Figure 7 shows double-step chronoamperograms of the modified electrode in the absence (curve *a*) and in the presence (curves *b–d*) of EG. The applied potential steps were 0.58 and 0.21 V versus Ag|AgCl|KCl (3 M) in anodic and cathodic directions, respectively. On the potential jump to the value of 0.21 V, negligible currents were passed in the presence of different concentrations of EG which imply the occurrence of irreversible electrooxidation process. As illustrated, the forward and backward potential step chronoamperometry of the modified electrode in the blank solution showed an almost equal charge which is consumed for oxidation and reduction of surface-confined $Ni(OH)_2$/NiOOH sites [Fig. 7 (Inset A, curve a')]. However, in the presence of EG, the charge value associated with the forward chronoamperometry, Q, is greater than that of the observed for the backward [Fig. 7 (Inset A, curve d')]. These results indicate the electrocatalytic ability of this modified electrode for the oxidation of EG in alkaline media.

The rate constant for the chemical reaction between EG and redox sites of Ni/PMT(TX-100)/MCPE can be evaluated by chronoamperometry according to the method described in Ref. [37]:

$$I_C/I_L = \gamma^{1/2}[\pi^{1/2}\mathrm{erf}\ (\gamma^{1/2}) + \exp(-\gamma)/\gamma^{1/2}] \quad (1)$$

where I_C is the catalytic current of the Ni/PMT(TX-100)/MCPE in the presence of EG and I_L is the limiting current

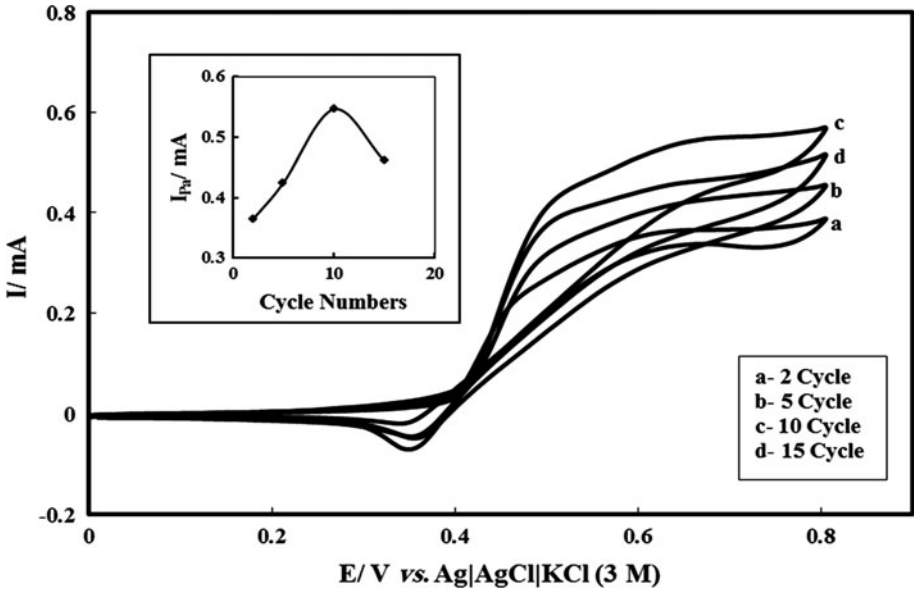

Fig. 8 Cyclic voltammograms of Ni/PMT(TX-100)/MCP electrodes prepared in cycle numbers in the range of 2–15 in modification steps and in the presence of 0.04 M of EG in 0.1 M of NaOH. *Inset* variation of electrocatalytic peak current of EG oxidation with cycle numbers. (t = 300 s, monomer concentration of 6.0 mM, TX-100 concentration of 6.0 mM, $NiSO_4$ concentration of 1.5 M, υ = 20 mV s^{-1})

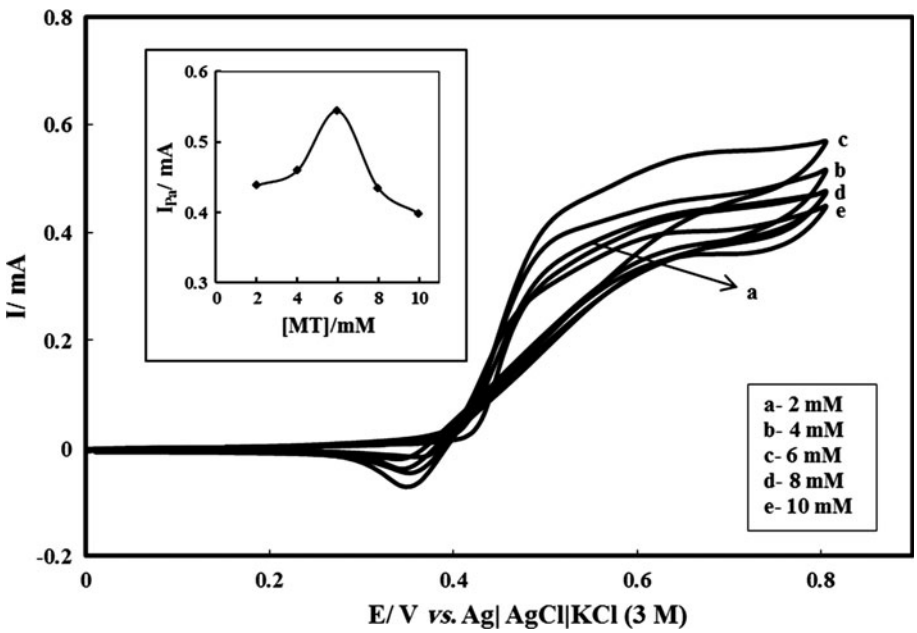

Fig. 9 Electrochemical responses obtained in 0.1 M of NaOH for Ni/PMT(TX-100)/MCP electrodes in the presence of 0.04 M of EG with monomer concentration in range of 2.0–10.0 mM in modification steps. *Inset* variation of anodic peak currents obtained with monomer concentration. (t = 300 s, cycle numbers: 10, TX-100 concentration of 6.0 mM, $NiSO_4$ concentration of 1.5 M and υ = 20 mV s^{-1})

in the absence of EG and $\gamma = kC_0t$ (C_0 is the bulk concentration of EG, mol cm^{-3}) is the argument of the error function. In cases where γ exceeds 2, the error function is almost equal to 1 and the above equation can be reduced to:

$$I_C/I_L = \pi^{1/2}\gamma^{1/2} = \pi^{1/2}(k\,C_0t)^{1/2} \quad (2)$$

where k, C_0, and t are the catalytic rate constant (cm^3 mol^{-1} s^{-1}), EG concentration (mol cm^{-3}), and the time elapsed (s), respectively. From the slope of I_C/I_L versus $t^{1/2}$ plot one can simply obtain the value of k for a given concentration of substrate. Inset B in Fig. 7 shows a plot constructed from the chronoamperograms of the Ni/PMT(TX-100)/MCPE in the absence and in the presence of 0.04 M EG. The calculated mean value of k was 2.1×10^6 cm^3 mol^{-1} s^{-1}.

3.6 Parameters affecting the electrode modification

3.6.1 *Effect of cycle number on the anodic peak current of EG*

Electrochemical polymerization offers the possibility to control the thickness and homogeneity of PMT film on the

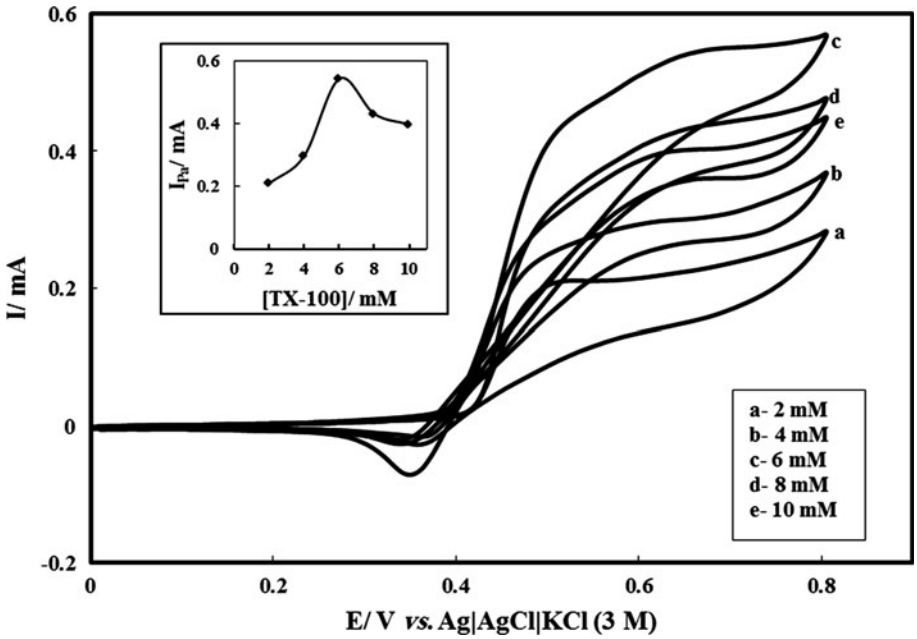

Fig. 10 Current–potential curves in 0.1 M of NaOH for Ni/PMT(TX-100)/MCP electrodes in the presence of 0.04 M of EG with TX-100 concentration in the range of 2.0–10.0 mM in modification steps. *Inset* variation of electrocatalytic peak current versus TX-100 concentration (t = 300 s, monomer concentration of 6.0 mM, cycle numbers: 10, $NiSO_4$ concentration of 1.5 M, υ = 20 mV s^{-1})

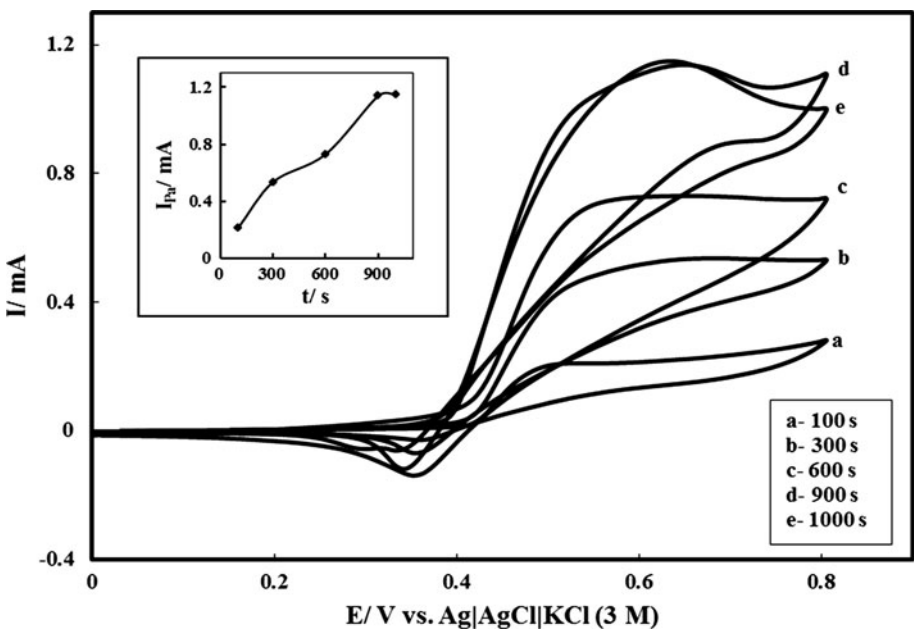

Fig. 11 Cyclic voltammograms of Ni/PMT(TX-100)/MCP electrodes prepared at various electrodepositing times in 0.1 M of NaOH solution, in the presence of 0.04 M of EG. *Inset* variation of the electrocatalytic peak current of EG versus time of plating (cycle numbers: 10, monomer concentration of 6.0 mM, TX-100 concentration of 6.0 mM, $NiSO_4$ concentration of 1.5 M, υ = 20 mV s^{-1})

electrode surface. The influence of the number of cycles required for the preparation of the PMT(TX-100) films on the electrocatalytic oxidation of EG was investigated and the corresponding results are shown in Fig. 8. Under the constant electrodepositing time of Ni, the anodic current rises progressively for the number of cycles up to ten cycles and drops afterward suggesting that the electrocatalysis of EG oxidation is sensitive to thickness of the polymer film. The increase in the anodic peak current for the number of cycles upto ten cycles may be due to the occupation of Ni in the pores of polymers with the real sizes. The decrease in anodic peak current for EG oxidation beyond ten cycles could be attributed to lessening of real surface area of Ni particles by the excessive presence of polymers on the electrode surface and the decrease of polymer conductivity at high thickness.

3.6.2 *Effect of monomer concentration*

The effect of MT monomer concentration on the reactivity of the Ni/PMT(TX-100)/MCPE for EG oxidation was investigated. Thus, different PMT(TX-100) films were prepared via electropolymerization of MT monomer in the solution with various concentrations in the range of 2.0–10.0 mM. After deposition of Ni particles into the obtained PMT/(TX-100) films, electrocatalytic capability of these modified electrodes for EG oxidation was investigated (Fig. 9). As can be seen in this figure, by increasing the monomer concentration from 2.0 to 6.0 mM, electrooxidation peak current of EG increased accordingly. Whereas in monomer concentration higher than 6.0 mM, electrooxidation peak current decreased. This phenomena may be attributed to the simultaneous formation of some oligomers during the polymerization of MT in high concentrations. Thus, the formation of the oligomers can affect the morphology of the polymer film which decreases the amount of Ni particles dispersed in the film. It also decreases the effective surface area of the catalyst, and, therefore, influences the poisoning extent via adsorption of some EG oxidation intermediates.

3.6.3 *Effect of TX-100 concentration*

According to literature, surfactants play a very important role in the electrodic reactions, not only in solubilizing organic compounds but also by providing specific orientation of the molecules at the electrode interface [38]. These molecules can give rise to adsorbed layers of varying thickness—monolayers, bilayers, or multilayers of a very complex structure [39] and thus affecting the rate of electrode reaction [40, 41]. Hence, in the present work, TX-100 was applied as a surfactant. In order to study the effect of varying concentrations of TX-100 on EG electrooxidation, the amount of anodic peak current was monitored as the index for finding optimum concentration. It is evident from Fig. 10 that the current increases up to 0.06 M of TX-100 and drops afterward. Therefore, concentration of 0.06 M of TX-100 was selected as the optimal level for preparation of Ni/PMT(TX-100)/MCPE.

3.6.4 *Effect of Ni electrodepositing time*

The peak current of EG oxidation depends largely on the amount of Ni incorporated into the film. The variation of the anodic peak current as a function of Ni electrodepositing time are presented in Fig. 11 (at electrodes with the

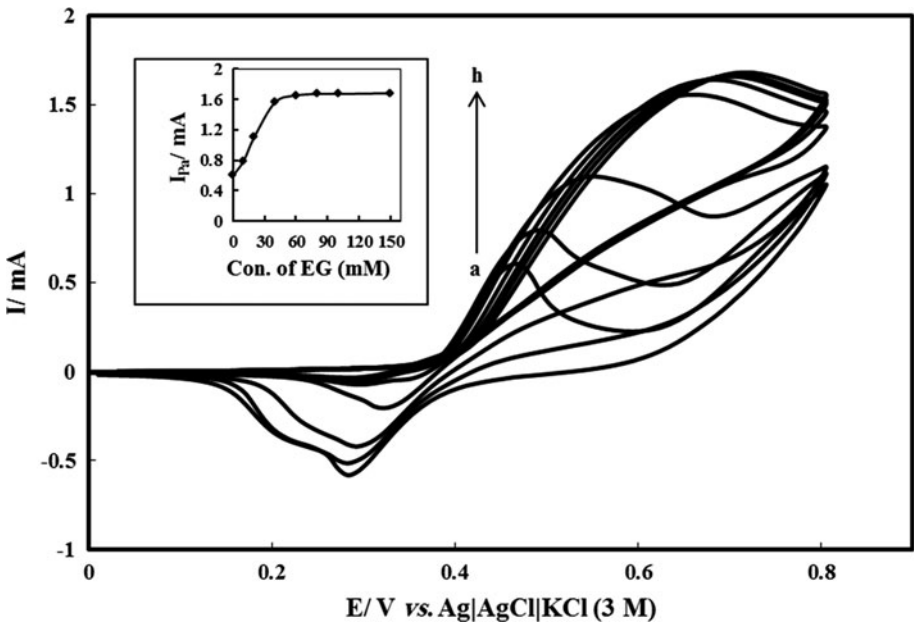

Fig. 12 Current–potential curves of 0.1 M of NaOH solution with different concentrations of EG *a* 0.0, *b* 0.01, *c* 0.02, *d* 0.04, *e* 0.06, *f* 0.08, *g* 0.1, and *h* 0.15 M at the Ni/PMT(TX-100)/MCPE at scan rate of 20 mV s^{-1}. *Inset* plot of the dependence of EG oxidation peak current on the EG concentration

same thickness of polymeric film). As shown in this figure, anodic peak current (I_{pa}) increases with increasing electrodepositing duration of Ni in the polymer film up to 900 s and remains almost constant afterward. This observation can be attributed to the saturation of active sites of the electrode surface at a longer duration. However, at lower durations, the area of Ni particles increases in proportion to the increase in the number of Ni particles and the electrocatalytic activity of the modified electrodes enhances.

3.6.5 *Effect of EG concentration*

Figure 12 shows cyclic voltammograms of Ni/PMT(TX-100)MCPE in the presence of various concentrations of EG in the range of 0.01–0.15 M. It is clearly observed that upon increasing EG concentration, its oxidation develops in the region of the electrochemical formation of Ni(III). Thus, it is likely that the Ni(III) species is the active moiety which efficiently speeds up the oxidation of EG.

In inset Fig. 12, it is clearly observed that the anodic current increases with increasing EG concentration and levels off at concentrations higher than 0.06 M. This effect is assumed to be due to the saturation of active sites at the surface of electrode. In accordance with this result, in order to obtain a higher peak current density, the optimum concentration of EG can be considered as about 0.06 M.

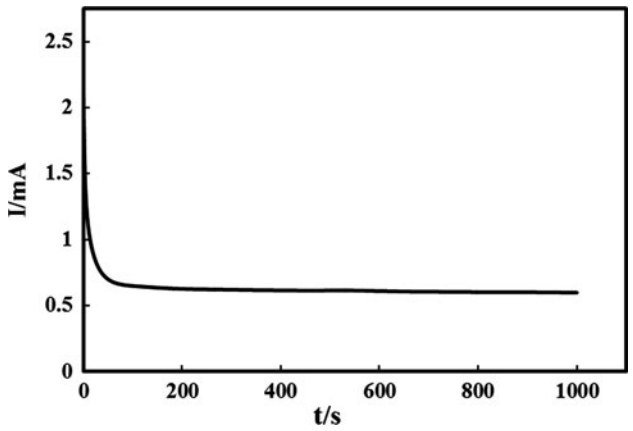

Fig. 13 Chronoamperometry of the $Ni(OH)_2$/PMT(TX-100)/MCPE in a solution of 0.1 M NaOH + 0.06 M EG. The electrode potential was held at 0.67 V for 1,000 s

3.7 Long-term stability of the $Ni(OH)_2$/PMT(TX-100)/MCPE

In the practical view, long-term stability of the electrode is important. The activity and stability of the $Ni(OH)_2$/PMT(TX-100)/MCPE was studied by using chronoamperometry method for a long time window in 0.1 M NaOH + 0.06 M EG solution (Fig. 13). As can be seen, the current density is decreased in the first few seconds and then reaches steady-state current density. It is obvious that the $Ni(OH)_2$/PMT(TX-100)/MCPE exhibits a good stability toward EG oxidation.

Finally, to evaluate the electrocatalytic activity of Ni/PMT(TX-100)/MCPE toward EG oxidation, the results obtained by this study were compared with those of similar research works in the literature (Table 1). As demonstrated in this table, the current density for oxidation of EG at the surface of Ni/PMT(TX-100)/MCPE is significantly higher than that previously reported by other research groups.

4 Conclusion

In this work, the PMT(TX-100)/MCPE was prepared by the electropolymerization of *m*-toluidine on a carbon paste electrode in the presence of TX-100. The electrochemical behavior of PMT(TX-100)/MCPE showed higher polymerization rate in the presence of TX-100 with a good electrical conductivity which could be due to the different morphology of PMT(TX-100)/MCPE. The Ni/PMT(TX-100)/MCPE was prepared by immobilization of Ni particles on the PMT(TX-100)/MCPE using electrodeposition of acidic Ni^{2+} solution. $Ni(OH)_2$ species onto the PMT(TX-100) film show higher electrocatalytic activity toward EG oxidation than that of the other Ni-modified electrodes. The kinetic parameters of EG such as charge-transfer coefficient and catalytic reaction rate constant for oxidation were determined using cyclic voltammetry and chronoamperometry techniques. The value for the rate

Table 1 Comparison of EG electrocatalytic oxidation at the surface of some modified electrodes

Modified electrode	EG concentration (M)	Scan rate (mV s^{-1})	j (mA cm^{-2})	E_p (V)	Reference electrode	Reference
Ni/SDS–PPAA/CPE	0.02	20	1.97	0.6	Ag|AgCl|KCl (3 M)	[23]
PolyNiTSPc/Au/Q	1	20	2.4	0.52	Ag|AgCl|KCl (sat'd)	[25]
Pt–Ru/CNT	0.5	50	1.5	0.66	Ag|AgCl|KCl (sat'd)	[42]
Pt/CNT	0.5	50	3.6	0.6	SCE	[43]
Ni/PMT(TX-100)/MCPE	0.06	20	6.9	0.67	Ag|AgCl|KCl (3 M)	This work

j Current density, E_p peak potential, *PPAA* poly(*p*-aminoacetanilide), *PolyNiTSPc* polynickeltetrasulfophthalocyanine

constant k (2.1×10^6 cm^3 mol^{-1} s^{-1}) obtained from the chronoamperometric method indicates that the modified electrode can overcome the kinetic limitations for EG oxidation by a catalytic process and can decrease the overpotential.

References

1. Dalbay N, Kadirgan F (1990) The properties of palladium electrodes for electrooxidation of ethylene glycol. J Electroanal Chem 296:559–569
2. Peled E, Livshits V, Duvdevani T (2002) High-power direct ethylene glycol fuel cell (DEGFC) based on nanoporous proton-conducting membrane (NP-PCM). J Power Sour 106:245–248
3. Livshits V, Peled E (2006) Progress in the development of a highpower, direct ethylene glycol fuel cell (DEGFC). J Power Sour 161:1187–1191
4. Matruoka K, Inaba M, Ogumi Z (2002) Anodic oxidation of polyhydric alcohols on a Pt electrode in alkaline solution. Fuel Cells 2:35–39
5. Livshits V, Philosoph M, Peled E (2008) Direct ethylene glycol fuel cell stack—study of oxidation intermediate products. J Power Sour 178:687–691
6. Demarconnay L, Coutanceau C, Lamy C, Leger JM (2006) Development of electrocatalysts for solid alkaline fuel cell (SAFC). J Power Sour 156:14–19
7. Hahn F, Beden B, Kadirgan F, Lamy C (1987) Electrocatalytic oxidation of ethylene glycol: Part III. In-situ infrared reflectance spectroscopic study of the strongly bound species resulting from its chemisorption at a platinum electrode in aqueous medium. J Electroanal Chem 216:169–180
8. Christensen PA, Hamnett A (1989) The oxidation of ethylene glycol at a platinum electrode in acid and base: an in situ FTIR study. J Electroanal Chem 260:347–359
9. Belgsir EM, Bouhier E, Essis Yei H, Kokoh KB, Beden B, Huser H, Leger JM, Lamy C (1991) Electrosynthesis in aqueous medium: a kinetic study of the electrocatalytic oxidation of oxygenated organic molecules. Electrochim Acta 36:1157–1164
10. Hauffe W, Heitbaum J (1978) The electrooxidation of ethylene glycol at platinum in potassium hydroxide. Electrochim Acta 23:299–304
11. Beden B, Kadirgan F, Kahyaoglu A, Lamy C (1982) Electrocatalytic oxidation of ethylene glycol in alkaline medium on paltinum–gold alloy electrodes modified by underpotential deposition of lead adatoms. J Electroanal Chem 135:234–329
12. Kadirgan F, Beden B, Lamy C (1983) Electrocatalytic oxidation of ethylene glycol: Part II. Behavior of platinum-ad-atom electrodes in alkaline medium. J Electroanal Chem 143:135–152
13. Kadirgan F, Bouhier-Charbonnier E, Lamy C, Leger JM, Beden B (1990) Mechanistic study of the electrooxidation of ethylene glycol on gold and adatom-modified gold electrodes in alkaline medium. J Electroanal Chem 286:41–61
14. Chang SC, Ho Y, Weaver MJ (1991) Applications of real-time FTIR spectroscopy to the elucidation of complex electroorganic pathways: electrooxidation of ethylene glycol on gold, platinum, and nickel in alkaline solution. J Am Chem Soc 113:9506–9513
15. Markovic NM, Avramov-Ivic ML, Marinkovic NS, Adzic RR (1991) Structural effects in electrocatalysis: ethylene glycol oxidation on platinum single-crystal surfaces. J Electroanal Chem 312:115–130
16. Zadeii JM, Marioli J, Kuwana T (1991) Electrochemical detector for liquid chromatographic determination of carbohydrates. Anal Chem 63:649–653
17. Ojani R, Raoof JB, Salmany-Afagh P (2004) Electrocatalytic oxidation of some carbohydrates by poly (1-naphthylamine)/nickel modified carbon paste electrode. J Electroanal Chem 571:1–8
18. Akhtar P, Too CO, Wallace GG (1997) Detection of amino acids at conducting electroactive polymer modified electrodes using flow injection analysis. Part I Use of macroelectrodes. Anal Chim Acta 339:201–209
19. Wen TC, Lin SM, Tsai JM (1994) Sulphur content and the hydrogen evolving activity of NiS_x deposits using statistical experimental strategies. J Appl Electrochem 24:233–238
20. Fan C, Piron DL, Sleb A, Paradis P (1994) Study of electrodeposited nickel-molybdenum, nickel-tungsten, cobalt-molybdenum, and cobalt-tungsten as hydrogen electrodes in alkaline water electrolysis technical papers—Electrochemical Science and Technology. J Electrochem Soc 141:382–387
21. Raj IA, Vasu KI (1990) Transition metal-based hydrogen electrodes in alkaline solution—electrocatalysis on nickel based binary alloy coatings. J Appl Electrochem 20:32–38
22. Casadei MA, Pletcher D (1988) The influence of conditions on the electrocatalytic hydrogenation of organic molecules. Electrochim Acta 33:117–120
23. Ojani R, Raoof JB, Rahemi V (2011) Evaluation of sodium dodecyl sulfate effect on electrocatalytic properties of poly (4-aminoacetanilide)/nickel modified carbon paste electrode as an efficient electrode toward oxidation of ethylene glycol. Int J Hydrogen Energy 36:13288–13294
24. Agboola B, Nyokong T (2007) Electrocatalytic oxidation of chlorophenols by electropolymerised nickel(II) tetrakis benzylmercapto and dodecylmercapto metallophthalocyanines complexes on gold electrodes. Electrochim Acta 52:5039–5045
25. Ureta-Zanartu MS, Alarcon A, Munoz G, Gutierrez C (2007) Electrooxidation of methanol and ethylene glycol on gold and on gold modified with an electrodeposited polyNiTSPc film. Electrochim Acta 52:7857–7864
26. Raoof JB, Ojani R, Hosseini SR (2011) A novel, effective and low cost catalyst for methanol oxidation based on nickel ions dispersed onto poly(*o*-toluidine)/Triton X-100 film at the surface of multi-walled carbon nanotube paste electrode. J Power Sour 196:1855–1863
27. Raoof JB, Ojani R, Hosseini SR (2011) Electrochemical fabrication of novel Pt/poly (*m*-toluidine)/Triton X-100 composite catalyst at the surface of carbon nanotube paste electrode and its application for methanol oxidation. Int J Hydrogen Energy 36:52–63
28. Raoof JB, Ojani R, Abdi S, Hosseini SR (2012) Highly improved electrooxidation of formaldehyde on nickel/poly (*o*-toluidine)/Triton X-100 film modified carbon nanotube paste electrode. Int J Hydrogen Energy 37:2137–2146
29. Inzelt G, Pireni M, Schultze JW, Vorotynstev MA (2000) Electron and proton conducting polymers: recent developments and prospects. Electrochim Acta 45:2403–2421
30. Carswell ADW, O'Rear EA, Grady BP (2003) Adsorbed surfactants as templates for the synthesis of morphologically controlled polyaniline and polypyrrole nanostructures on flat surfaces: from spheres to wires to flat films. J Am Chem Soc 125:14793–14800
31. Kohut-Svelko N, Reynaud S, Francois J (2005) Synthesis and characterization of polyaniline prepared in the presence of nonionic surfactants in an aqueous dispersion. Synth Met 150:107–114
32. Cai Z, Lei J, Liang W, Menon V, Martin CR (1991) Molecular and supermolecular origins of enhanced electric conductivity in templatesynthesized polyheterocyclic fibrils.1. Supermolecular effects. Chem Mater 3:960–967
33. Pham MT, Maitz MF, Richter E, Reuther H, Prokert F, Mucklich A (2004) Electrochemical behaviour of nickel surface-alloyed with copper and titanium. J Electroanal Chem 572:185–193

34. Majdi S, Jabbari A, Helli H, Moosavi-Movahedi AA (2007) Electrocatalytic oxidation of some amino acids on a nickel–curcumin complex modified glassy carbon electrode. J Electrochim Acta 52:4622–4629
35. Hajjizadeh M, Jabbari A, Heli H, Moosavi-Movahedi AA, Shafiee AA, Karimian K (2008) Electrocatalytic oxidation and determination of deferasirox and deferiprone on a nickel. Anal Biochem 373:337–348
36. Raoof JB, Karimi MA, Hosseini SR, Mangelizade S (2011) Enhanced electrocatalytic activity of nickel particles electrodeposited onto poly (*m*-toluidine) film prepared in presence of CTAB surfactant on carbon paste electrode for formaldehyde oxidation in alkaline medium. Int J Hydrogen Energy 36: 13281–13287
37. Bard AJ, Faulkner LR (2001) Electrochemical methods. Wiley, New York
38. Westmoreland PG, Day RA, Underwood A (1972) Electrochemistry of substances solubilized in micelles. Polarography of azobenzene in aqueous surfactant solutions. Anal Chem 44: 737–740
39. Rosen MJ (1978) Surfactants and interfacial phenomena. Wiley Interscience, New York
40. Oshsawa Y, Aoyagui S (1982) A correlation between the half-wave potential and the micelle-solubilization equilibrium of ferrocene in cationic micellar solutions. J Electroanal Chem 136:353–360
41. Quintela PA, Kaifer AE (1987) The electrochemistry of methylviologen in the presence of sodium decyl sulfate. Langmuir 3:769–773
42. Maxakato NW, Arendse CJ, Ozoemena KI (2009) Insights into the electro-oxidation of ethylene glycol at Pt/Ru nanocatalysts supported on MWCNTs: Adsorption-controlled electrode kinetics. Electrochem Commun 11:534–537
43. Selvaraj V, Vinoba M, Alagar M (2008) Electrocatalytic oxidation of ethylene glycol on Pt and Pt–Ru nanoparticles modified multi-walled carbon nanotubes. J Colloid Interface Sci 322: 537–544